l'Observatoire de Paris — SYRTE — Systèmes de Référence Temps-Espace | LNE — Le progrès, une passion à partager | CNRS — CENTRE NATIONAL DE LA RECHERCHE SCIENTIFIQUE

FREQUENCY COMPARISON (H_MASER 40 0890) - (LNE-SYRTE-FO2)
From MJD 53639 to MJD 53664

The primary frequency standard LNE-SYRTE-FO2 was compared to the hydrogen Maser (40 0890) of the laboratory, from MJD 53639 to MJD 53664.

The mean frequency differences measured between the hydrogen Maser 40 0890 and fountain FO2 during this period is given in table 1.

Period (MJD)	**y(HMaser$_{40\ 0890}$ - FO2)** (7)	u_B (2)	u_A (7)	$u_{link\ /\ maser}$ (4)
53639 – 53664	**-1332,07**	**5,78**	**0,71**	**1,43**

Table 1: Results of the comparison in 1 x 10^{-16} unit.

Figure 1 collects the measurements of fractional frequency differences during the 26th September to 21st October 2005 period. Error bars represent the combined statistical and systematic uncertainties. The measurements are corrected for the systematic frequency shifts listed below.

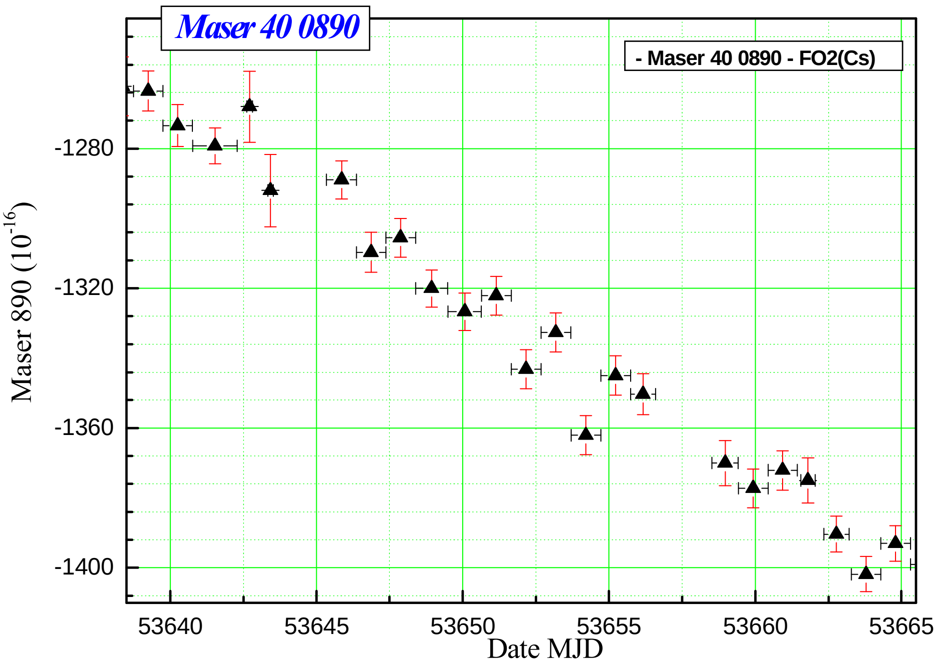

Figure 1: fractional frequency differences between H_Maser40 0890 & FO2 from MJD 53639 to MJD 53664

Table of measurements is given bellow (table 2) and a synthesis of calculation on table 3.

Hydrogen Maser 40 0890 stability against Hydrogen Maser 40 0889

During the period 53639 – 53664 hydrogen maser 40 0889 and hydrogen maser 40 0890 were compared. Phase differences between masers 40 0889 and 40 0890 were measured each hour. Figure 2 represents the measurements after quadratic fit removed from phase data and figure 3 represents the frequency stability of phase differences drift removed. These figures show the very good stability of maser 40 0889 and 400890 during this period of measurement.

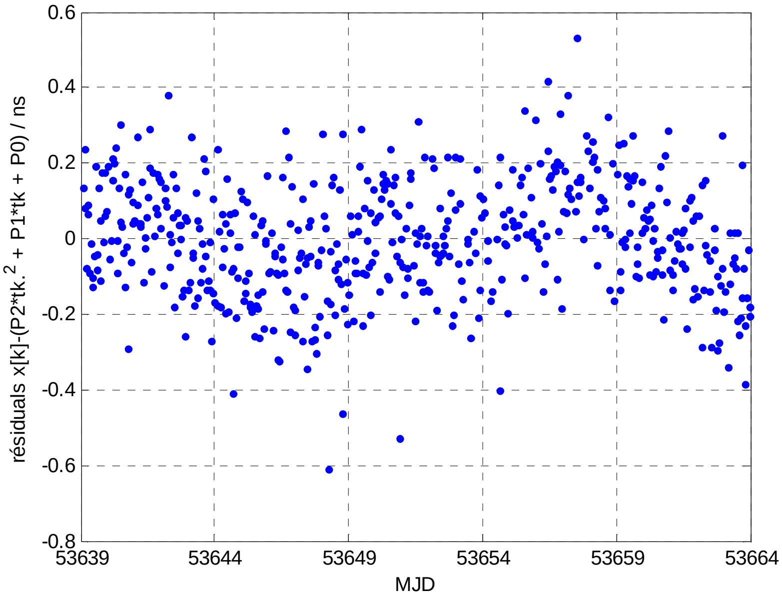

Figure 2: phase differences quadratic fit removed between H_Maser40 0889 & H_Maser40 0890 from MJD 53639 to MJD 53664

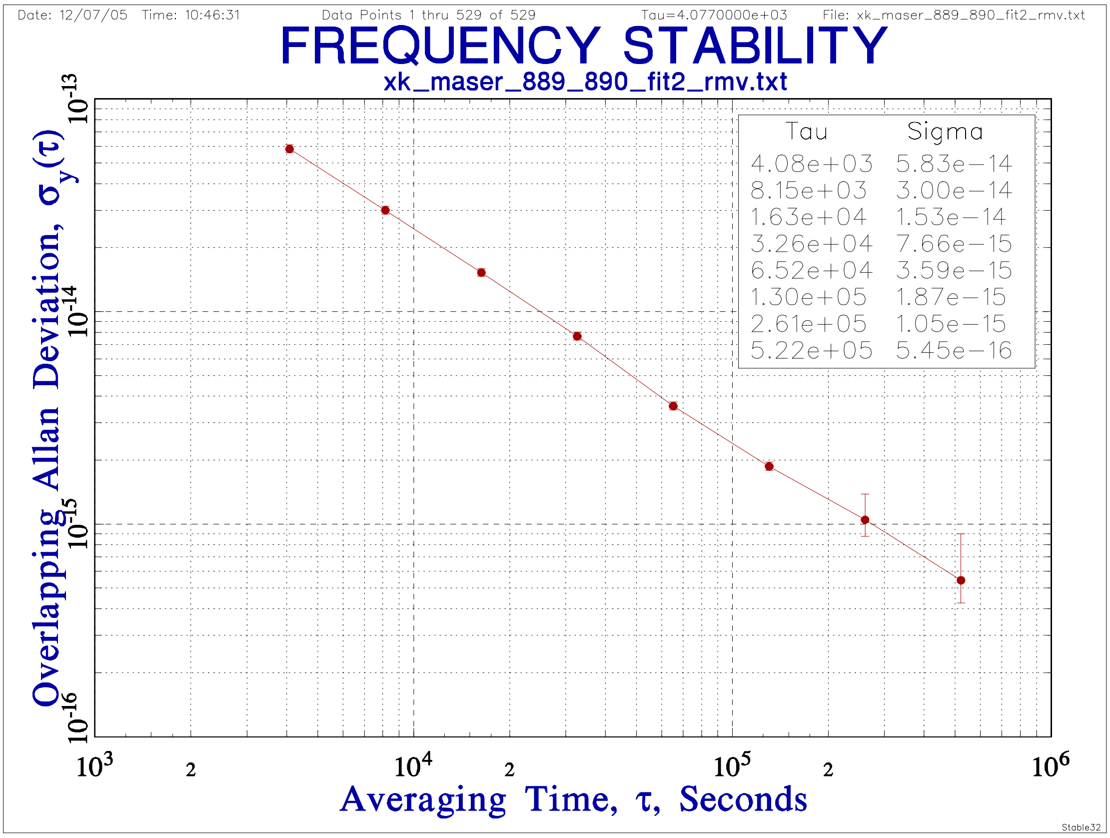

Figure 3: frequency stability of phase differences between H_Maser40 0889 & H_Maser40 0890 from MJD 53639 to MJD 53664

Hydrogen Maser 40 0890 stability against fountain clock FO2

By using all cycle by cycle maser 40 0890 against FO2 measurements from MJD 53636 to MJD 53667 we obtain un chronological time series of 1670634 samples regularly spaced by the average of 1.6 second. A linear frequency drift is removed from the data $y_k = a_1 + a_2\, t$ as it is mentioned in Annex 4. The stability analysis is realized by the computation of the overlapping Allan deviation over the average chronological time series with a factor of 2 (due to the number of data limited by the software). The time interval between consecutively measurements is 3,2 seconds and the number of sampled measurements is 835317. Figure 3 bis represents the frequency stability obtained and shows that a stability of $3\text{x}10^{-16}$ is reached at five days.

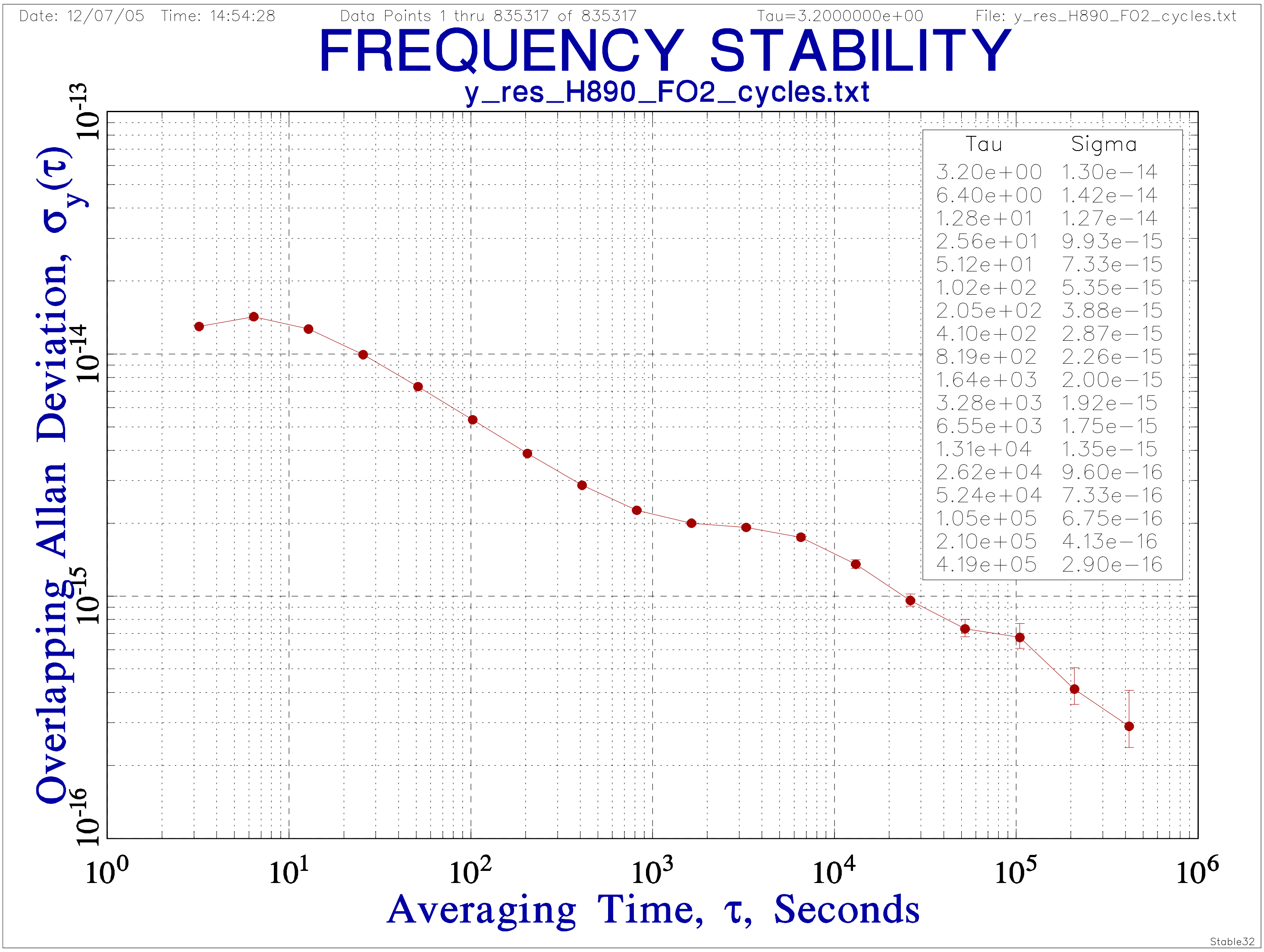

Figure 3_bis: frequency stability of frequency differences between H_Maser40 0890 & FO2fountain clock from MJD 53636 to MJD 53667

Start UTC dates unit MJD	Start Local dates unit H:M	Duration H :M	Mean fractional frequency differences $y_{Maser} - y_{FO2}$	type A uncertainties σ_{Stat}	$\sigma_{Collision}$
53638,74054398	25/09/2005 19:46	24:20	-1,263547E-13	2,68E-16	3,16E-16
53639,75458333	26/09/2005 20:06	24:12	-1,273463E-13	2,96E-16	3,5E-16
53640,77268519	27/09/2005 20:32	36:28	-1,279214E-13	2,11E-16	2,51E-16
53642,61597222	29/09/2005 16:47	04:45	-1,268033E-13	5,99E-16	7,12E-16
53643,32968750	30/09/2005 09:54	04:37	-1,292021E-13	5,86E-16	7,53E-16
53645,34740741	02/10/2005 10:20	24:25	-1,289001E-13	2,42E-16	2,94E-16
53646,36494213	03/10/2005 10:45	23:58	-1,309698E-13	2,65E-16	3,23E-16
53647,36361111	04/10/2005 10:43	24:28	-1,305570E-13	2,48E-16	3,04E-16
53648,38978009	05/10/2005 11:21	26:17	-1,320066E-13	2,29E-16	2,77E-16
53649,49753472	06/10/2005 13:56	27:21	-1,326730E-13	2,29E-16	2,74E-16
53650,63896991	07/10/2005 17:20	24:24	-1,322103E-13	2,47E-16	3E-16
53651,65562500	08/10/2005 17:44	24:30	-1,343160E-13	2,57E-16	3,03E-16
53652,67697917	09/10/2005 18:14	24:28	-1,332665E-13	2,53E-16	3,04E-16
53653,70666667	10/10/2005 18:57	24:26	-1,362113E-13	2,55E-16	3,04E-16
53654,72471065	11/10/2005 19:23	24:19	-1,345010E-13	2,59E-16	3,1E-16
53655,73775463	12/10/2005 19:42	20:32	-1,350316E-13	2,8E-16	3,33E-16
53658,52097222	15/10/2005 14:30	21:34	-1,370047E-13	3,24E-16	3,89E-16
53659,42524306	16/10/2005 12:12	24:30	-1,377273E-13	2,5E-16	3,01E-16
53660,44607639	17/10/2005 12:42	23:50	-1,372098E-13	2,51E-16	3,13E-16
53661,55688657	18/10/2005 15:21	11:46	-1,375000E-13	3,61E-16	4,34E-16
53662,33784722	19/10/2005 10:06	20:48	-1,390377E-13	2,6E-16	3,2E-16
53663,28493056	20/10/2005 08:50	24:16	-1,401832E-13	2,53E-16	3,04E-16
53664,29584491	21/10/2005 09:06	24:17	-1,393026E-13	2,57E-16	3,13E-16

Table 2: Measurements H_Maser40 0890 - FO2 from MJD 53639 to 53664

Dates Duration & Measurement Rate	Mean frequency difference normalized $y_{Maser} - y_{FO2}$	type A uncertainty σ_{Stat} & $\sigma_{Collision}$	Uncertainty due to the dead times $\sigma_{deadTime}$ **(4)**
Start date MJD UTC 53638,74054 Stop date MJD UTC 53665,30764 Total duration : 26,567 d Total measurements 21,43 d Measurement Rate: 80,67 %	Standard Mean **(1)** $\bar{y}$ = **-1333,14 x 10^{-16}** Weighted Mean **(5)**: $\bar{y}$ = **-1334,66 x 10^{-16}** Linear fit regression **(6)**: $\bar{y}$ = **-1332,57 x 10^{-16}** High order polynomial fit **(6)**: $\bar{y}$ = **-1333,18x 10^{-16}** Mean from Phase differences **(7)**: $\bar{y}$ = **-1332,07 x 10^{-16}**	Standard deviation s_y = 42,**83** x **10^{-16}** By Weighted Mean **(5)** σ_A = 0,**87** x **10^{-16}** By Linear fit regression**(6)** σ_y = 0,**87** x **10^{-16}** By High order Polynomial fit **(6)** u_A = 0,**89** x **10^{-16}** From Phase differences **(7)** σ_A = 0,**71** x **10^{-16}**	$\sigma_{deadTime}$ = **1,02 10^{-16}**

Table 3: Statistics of measurements

(1) Fractional frequency difference obtained after systematic relative frequency shifts correction:

$$y_{Maser-FO2} = \frac{(\delta(\nu))_{Zeeman2}}{\nu_0} + \frac{(\delta(\nu))_{BlackBody}}{\nu_0} + \frac{(\delta(\nu))_{Collision+CavityPulling}}{\nu_0} + \frac{(\delta(\nu))_{redshift}}{\nu_0} - \frac{f_{mesure}}{\nu_0}$$

with $\nu_0 := 0.9192631770 \; 10^{10}$. The fractional frequency mean is calculated by four ways as mentioned in table 3 in order to have comparison between statistical computation such as standard mean, weighted mean, with a linear fit and with phase differences.

(2) Systematic uncertainty $\sigma_B = u_B$ in which statistical effect of cold collisions and cavity pulling is removed (see **Annex 1**)

$$\sigma_B = \left(\sigma_{Zeeman2}^{\;2} + \sigma_{BlackBody}^{\;2} + \sigma_{Collision_{Syst}}^{\;2} + \sigma_{Microwave\_Spectrum}^{\;2} + \sigma_{Microwave\_Leakage}^{\;2} + \sigma_{Ramsey\_Rabi}^{\;2} + \sigma_{Recoil}^{\;2} + \sigma_{second\_Doppler}^{\;2} + \sigma_{Background\_collsions}^{\;2} + \sigma_{Redshift}^{\;2}\right)^{(1/2)}$$

(3) Statistical uncertainty $\sigma_A = u_A$, in which is taken into account the statistical uncertainty on each measurement σ_{Stat_i} and statistical effect on the cold collisions and Cavity Pulling measurement $\sigma_{Collision_i}$ (see **Annex 4** Linear Regression on the frequency measurements & **Annex 5**) : $\sigma_A = \sqrt{\dfrac{1}{\sum_{i=1}^{n} \dfrac{1}{\sigma_{Stat_i}^{\;2} + \sigma_{Collision_i}^{\;2}}}}$

(4) Uncertainty due to the link between H_Maser and the fountain FO2 $u_{link\_Maser} = \sqrt{\sigma_{link\_Lab}^{\;2} + \sigma_{dead\_time}^{\;2}}$ where $\sigma_{link\_Lab} = 0.1 \; 10^{-15}$ and σ_{dead_time} is the uncertainty due to the dead times during measurements (see **Annex 3**)

(5) Weighted Mean by statistical uncertainty on each measurement

$$y_j := \frac{\sum_{i=1}^{n_j} \frac{y_i}{\sigma_{Ai}^{\;2}}}{\sum_{i=1}^{n_j} \frac{1}{\sigma_{Ai}^{\;2}}}$$

where $\sigma_A = \sqrt{\dfrac{1}{\sum_{i=1}^{n} \dfrac{1}{\sigma_{A_i}^{\;2}}}}$ with $\sigma_{A_i} = \sqrt{\sigma_{Stat_i}^{\;2} + \sigma_{Collision_i}^{\;2}}$

(6) Mean frequency obtained by a linear fit by weighted least squares with statistical uncertainty on each measurement and by a high order polynomial fit (see **Annex 4**).

(7) Mean frequency obtained by phase differences that is the retained result (see **Annex 5**).

ANNEX 1

Uncertainties of systematic effects in the FO2 fountain

Systematic effects taken into account are the quadratic Zeeman, the Black Body, the cold collision and cavity pulling corresponding to the systematic part (see Annex 2), the microwave spectral purity and the microwave leakage, the Ramsey Rabi pulling, the recoil, the 2nd Doppler and the background collisions. Each of these effects is affected by an uncertainty. The uncertainty of the red shift effect is also included in the systematic uncertainty budget and gives

$$\sigma_B = \left(\sigma_{Zeeman2}{}^2 + \sigma_{BlackBody}{}^2 + \sigma_{Collision_{Syst}}{}^2 + \sigma_{Microwave\_Spectrum\_Leakage}{}^2 + \sigma_{first\_Doppler}{}^2 + \sigma_{Ramsey\_Rabi}{}^2 + \sigma_{Recoil}{}^2 + \sigma_{second\_Doppler}{}^2 + \sigma_{Background\_collisions}{}^2 + \sigma_{Redshift}{}^2 \right)^{(1/2)}$$

Here are mentioned the uncertainties of the different effects (see **Annex 2** and **[ref, 1]**):

Quadratic Zeeman effect	:	$\sigma_{Zeeman2} = 7.702\ 10^{-18}$	(continuously measured)
Black Body effect	:	$\sigma_{BlackBody} := 6.\ 10^{-17}$	(calculated)
Systematic Collisional effect	:	$\sigma_{Collision_{Syst}} := 9.3\ 10^{-17}$	(continuously measured see annex 2)
Microwave Spectrum purity & Leakage effect	:	$\sigma_{Microwave\_Spectrum\_Leakage} := 4.4\ 10^{-16}$	(measured)
First order Doppler effect	:	$\sigma_{first\_Doppler} := 3.0\ 10^{-16}$	(calculated and measured)
Rabi-Ramsey effect	:	$\sigma_{Ramsey\_Rabi} < 1.0\ 10^{-16}$	(calculated)
Recoil effect (see **[ref, 3]**)	:	$\sigma_{Recoil} := 1.0\ 10^{-16}$	(calculated)
Second order Doppler effect	:	$\sigma_{second\_Doppler} := 8.\ 10^{-18}$	(calculated)
Background effect	:	$\sigma_{Background\_collisions} := 1.0\ 10^{-16}$	(evaluated)
Red shift effect	:	$\sigma_{Redshift} := 1.0\ 10^{-16}$	(calculated)

For the whole September-October 2005 period it gives

➔ $$\boxed{\sigma_B = 5.78\ 10^{-16}}$$

1 - Measurement of the 2nd order Zeeman frequency shift

Every 20 minutes the frequency of the central fringe of the field linearly dependant transition |F=3, m_F=1⟩ ⟶ |F=4, m_F=1⟩ is measured. This frequency is directly proportional to the field as $\delta(\nu_{11})=K_{Z1}B$ with K_{Z1} = 7,0084 Hz.nT^{-1} (see **[ref. 5]** vol. 1 p37 table 1.1.7(a)). In the fountain, the transition |F=3, m_F=0⟩ ⟶ |F=4, m_F=0⟩ is shifted by quadratic Zeeman effect and depend on squared magnetic field as $\delta(\nu_{00})=K_{Z2}B^2$ with K_{Z2} = 42,745 mHz.µT^{-2} (see **[ref. 5]** vol. 1 p37 table 1.1.7(a)). Knowing K_{Z1} and measuring δ(ν11) allow good estimation of Zeeman quadratic shift as $\delta(\nu_{00})=K_{Z2}\left(\frac{\delta(\nu_{11})}{K_{Z1}}\right)^2$. The relative quadratic Zeeman frequency shift is calculated by $\frac{\delta(\nu_{00})}{\nu_0}=427{,}45\times10^{-6}\left(\frac{\delta(\nu_{11})}{700{,}84}\right)^2$ with $\delta(\nu_{11})$ in Hz unit and ν_0 = 9192631770 Hz. And the uncertainty is evaluated by $\frac{\Delta(\delta(\nu_{00}))}{\nu_0}=427{,}45\times10^{-6}\times\frac{2\times\overline{B}\times\Delta(B)}{\nu_0}$ with $B=M1/K_{Z1}$ in mG. Figure 4 displays the tracking of the central fringe *M1* during MJD 53639 to MJD 53665. This shows the good stability of the magnetic field in the interrogation zone. The frequency variation is taken as in an interval of standard deviation ± $\Delta M1 = 0{,}02864385$ **Hz**. When taking the standard deviation of variation of the magnetic field Δ(*B*) over the whole measurement period as the field uncertainty, we find **4,087** pT. The corresponding uncertainty of the correction of the second order Zeeman effect is **0,077x10^{-16}**. During each period of about 24h of integration (see table 2) an evaluation of the Zeeman effect is calculated assorted with an uncertainty averaged from the tracking of the central fringe during this interval duration of about 24h.

For central fringe center averaged $M1 = 1420.20726$ Hz, relative quadratic Zeeman shift $\frac{(\delta(f))_{Zeeman2}}{\nu_0}=\frac{K_{Z_2}M1^2}{K_{Z_1}^2\nu_0}$, with a average of $\frac{(\delta(f))_{Zeeman2}}{\nu_0}=1.90946\ 10^{-13}$ and an uncertainty $\sigma\left(\frac{(\delta(f))_{Zeeman2}}{\nu_0}\right)=\frac{2K_{Z_2}B\,\delta(B)}{\nu_0}$ giving $\sigma_{Zeeman2}=7.702\ 10^{-18}$

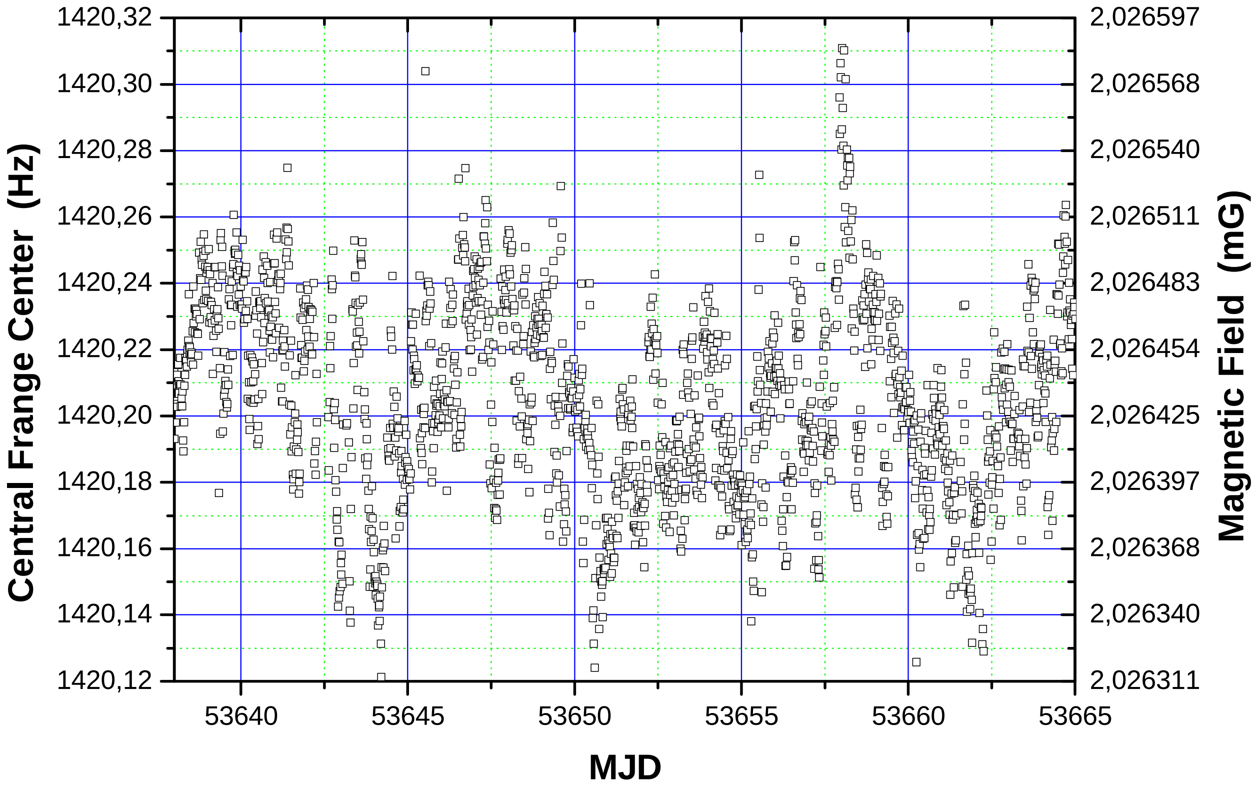

Figure 4: tracking of the central fringe from MJD 53639 to MJD 53565

2 - Measurement of the Blackbody Radiation shift

An ensemble of 3 platinum thermistors monitors the temperature and its gradient inside the vacuum chamber. The average temperature is T~24,63°C with a gradient smaller than $\delta(T) = 0.2\ K$ along the atom trajectory. The correction is

$$\left(\frac{\delta(\nu)}{\nu_0}\right)_{Blackbody} = \frac{K_{BB}\, T^4 \left(1 + \frac{\varepsilon\, T^2}{T_0^2}\right)}{T_0^4}$$

with $K_{BB} := -1.711\ 10^{-14} \& + \text{-}3.2\ 10^{-17}$ **[ref. 10]**, $\varepsilon := 0.014 \& + \text{-}0.0014$ **[ref. 11,12]**, $T_0 := 300\ K$. The Blackbody Radiation shift is assorted of uncertainty obtained with the squared of quadratic sum of $\delta(K_{BB})$, $\delta(\varepsilon)$ and $\delta(T)$:

$$\left(\frac{\delta(\nu)}{\nu_0}\right)_{Blackbody} = -1.6841\ 10^{-14} \pm 6.\ 10^{-17}$$

3 - Measurement of the collisional frequency shift and the cavity pulling

Collisional shift takes into account the effect of the collisions between cold Caesium atoms and the effect of "Cavity Pulling" whose influence also depends on the number of atoms. This effect is measured in a differential way during each integration and its determination thus depends on the duration of the measurement and on the stability of the clock, thus the uncertainty on the determination of the collisional shift is mainly of statistical nature. To the statistical uncertainty, we add a type B uncertainty of 1% of frequency shift resulting from the imperfection of the adiabatic passage method (see the article **[ref. 4]**).

Figure 5 visualizes the relative frequency shift due to the effect of the collisions and "Cavity Pulling" of the atomic fountain FO2 taken in low density, between the MJD 53639 and 53664 with the statistical uncertainty of each measurement, $\sigma_{Collision(i)}$ given in table 2.

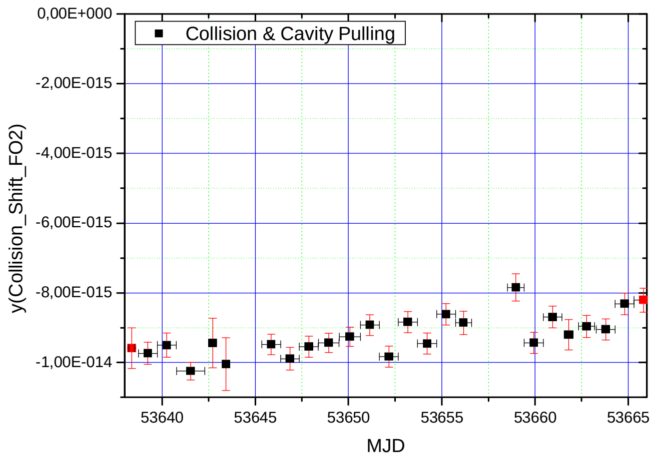

Figure 5: Fractional frequency shift due to cold collisions and Cavity Pulling from MJD 53639 to MJD 53664

The weighted mean $y_{Collision_{moy}} = \dfrac{\sum_{i=1}^{n} \dfrac{y_{Collision_i}}{\sigma_{Collision_i}^2}}{\sum_{i=1}^{n} \dfrac{1}{\sigma_{Collision_i}^2}}$ of collisionnal shift gives for September October: $(y_{Collision})_{moy} = -9.2590\ 10^{-15}$.

The systematic effect of these shifts is evaluated by the 1% part of the mean frequency collisional shift during September October 2005:

$$\sigma_{Collision_{Syst}} = \frac{1}{100}\left|y_{Collision_{moy}}\right| = \quad \sigma_{Collision_{Syst}} := 9.2590\ 10^{-17}$$

This value is taking into account in the systematic uncertainty evaluation σ_B (see Annex 1).

4 - Effect of the Microwave Spectrum effect and leakage effect

The clock frequency is measured as a function of the microwave power. Every 50 cycles the atom interrogation is alternated between 4 configurations of π/2, low density and high density, and 3π/2, low density and high density. It allows extrapolating and removing the variation of the collision shift in the comparison between π/2 and 3π/2 pulses. We find

$$\frac{(\delta(\nu))_{Microwave\_Spectrum\_Leakage}}{\nu_0} = -4.4\ 10^{-16} \pm \quad 3.3\ 10^{-16}$$

5 - Measurement of the residual 1st order Doppler effect

We determined the frequency shifts caused by asymmetry of the coupling coefficients of the two microwave feedthroughs and the error on the launching direction by coupling the interrogation signal either "from the right" or "from the left" or symmetrically into the cavity. The measured shift is

$$\left(\frac{\delta(\nu)}{\nu_0}\right)_{first\_Doppler} = 4.5\ 10^{-15} \pm \quad 1.1\ 10^{-16}$$

In FO2 fountain we feed the cavity symmetrically at 1% level both in phase and in amplitude. This shift is thus reduced by a factor of 100 and becomes negligible. The quadratic dependence of the phase becomes dominant. A worse case estimate based on **[ref. 6]** gives fractional frequency shift of 3 x 10^{-16} which we take as uncertainty due to the residual 1st order Doppler effect.

6 – Rabi and Ramsey effect and Majorana transitions effect

An imbalance between the residual populations and coherences of $m_F < 0$ and $m_F > 0$ states can lead to a shift of the clock frequency estimated to few 10^{-18} for a population imbalance of 10^{-3} that we observe in FO2 (see **[ref. 7]** and **[ref. 8]**).

7 – Microwave recoil effect

The shift due to the microwave photon recoil was investigated in **[ref. 3]**. It is smaller than 1,4 x 10^{-16} .

8 – Gravitational red-shift and 2nd order Doppler shift

The relativistic effect is evaluated as: $\frac{\delta(\nu)_{redshift}}{\nu_0} = 0.625\ \ 10^{-14}$ with an uncertainty $\sigma_{Redshift} = 0.1\ \ 10^{-15}$

The 2nd order Doppler shift is less than 0,08 x 10^{-16} .

9 – Background collisions effect

The vacuum pressure inside the fountains is typically a few 10^{-8} Pa. Based on early measurements of pressure shift (see **[ref. 5]**) the frequency shift due to collisions with the background gas is < 10^{-16}.

See **[ref. 9]** for recent evaluations of systematic effects of FO2 fountain.

Uncertainty due to the dead time during the measurements

A statement of the distribution of the idle periods of measurements of FO2 is represented in figure 6,

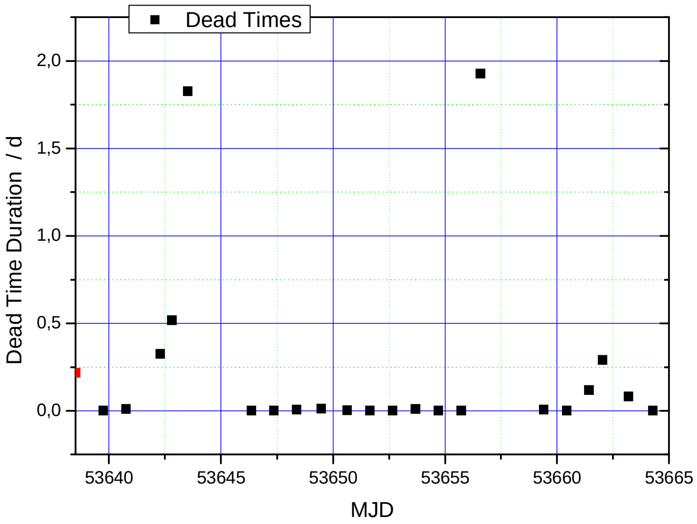

Figure 6: Dead Times on measurements of y(H_ Maser40 0890 –FO2) over the period MJD 53639 to 53664

For the period of the MJD 53623 until the MJD 53678 (10th September to 4th November 2005), the variations of phase between hydrogen Maser 40 0890 and the hydrogen Maser 40 0805 were sampled every 100s. After removing a quadratic fit on phase variations and eliminated outliers ±5σ to carry out the calculation of standard deviation in the temporal field, we have evaluated the uncertainty associated with the H_Maser according to time (by step of 100s). We have obtained the phase variations between H_Maser 40 0890 and the H_Maser 40 0805 plotted in figure 7.

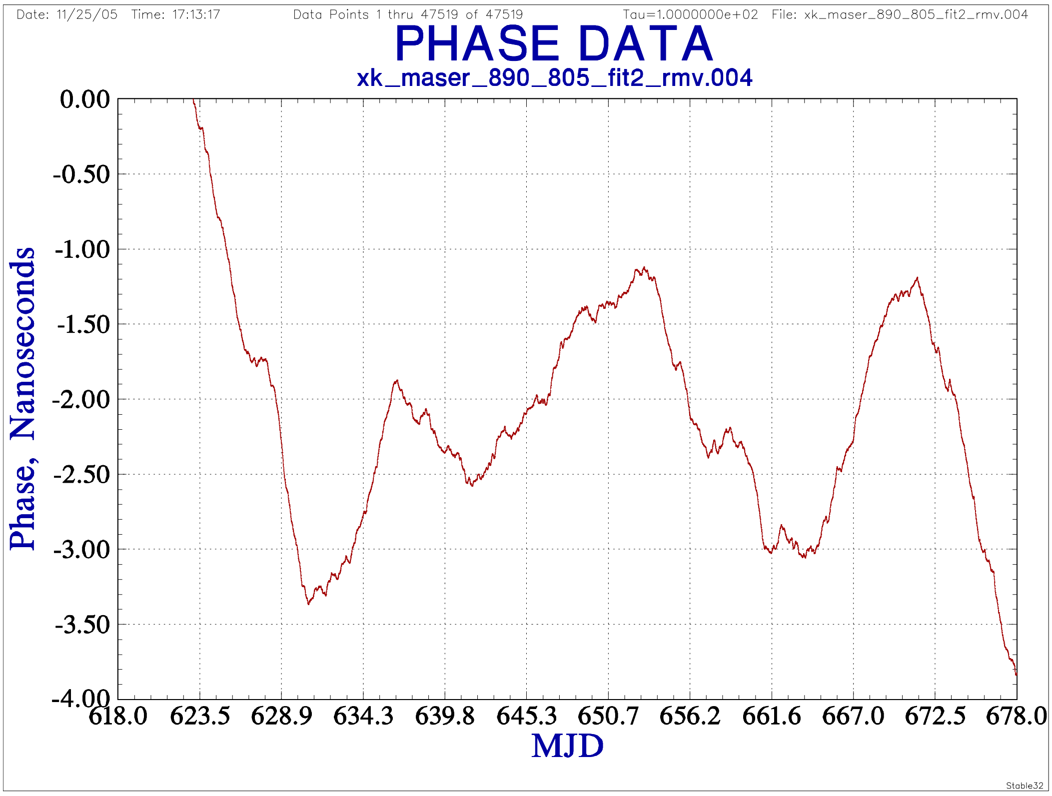

Figure 7: phase data x(Maser889-Maser890) quadratic fit removed x(H890-H805) MJD 53623 to MJD 53678

Frequency stability analyses were performed using the overlapping Allan deviation on frequency data and represented from 10th September to 4th November 2005 in figure 8 and similarly time stability analyses with a time deviation were computed and represented in figure 9.

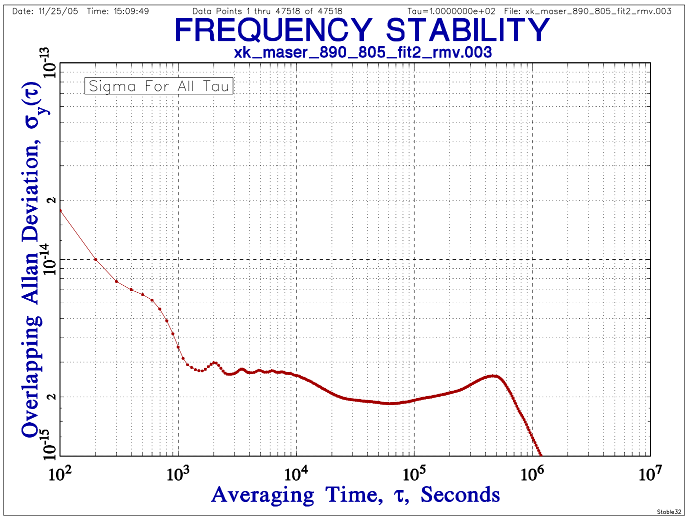

Figure 8: frequency stability analyzes x(HMaser890 - HMaser805) from MJD 53623 to MJD 53678

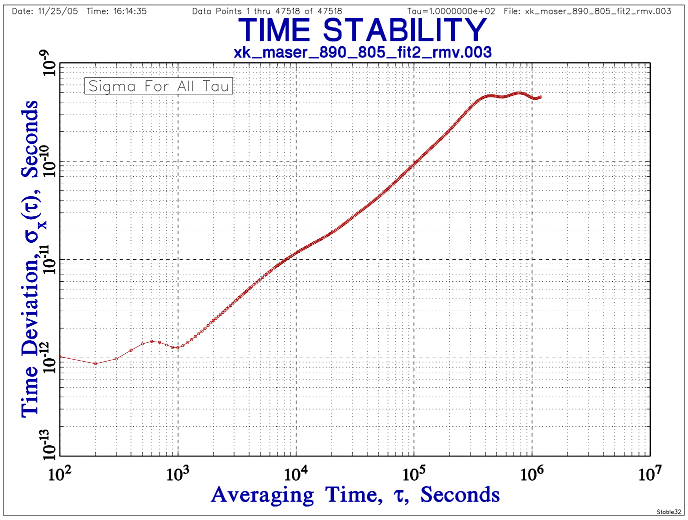

Figure 9: time stability analyzes from x(HMaser890 - HMaser805) from MJD 53623 to MJD 53678

Table 4 provides the standard deviations of the phase fluctuations of the hydrogen Maser 40 0890 with respect to the hydrogen Maser 40 0805 associated to each dead time according to their duration. The quadratic sum gives

$$\sum_{i=1}^{23} \sigma_x(\tau_m(i))^2 = 5.525477070\ 10^{-20}$$

The September October 2005 period of FO2 measurements is 26.567 days or $T = 2295397$ seconds. We find the standard deviation of the fluctuations of frequency due to the dead times in measurements by the ratio

$$\sigma_{deadTime} = \frac{\sqrt{\sum_{i=1}^{23} \sigma_{x_i}(\tau)^2}}{T} = \boxed{\sigma_{deadTime} := 1.024\ 10^{-16}}$$

End Date of each measurement (MJD)	Dead Time Duration $\tau_m(i)$ second	$\sigma_x(\tau_m(i))$ second
53639,75416667	36,000021617	0,000000000001025
53640,76250000	880,000024033	0,000000000001275
53642,29166667	28020,000013383	0,000000000025138
53642,81388889	44565,000007278	0,000000000039159
53643,52152778	157756,000030087	0,00000000015736
53646,36458333	31,000026735	0,000000000001025
53647,36319444	36,000019731	0,000000000001025
53648,38263889	616,999999015	0,000000000001469
53649,48472222	1107,000001660	0,000000000001328
53650,63680556	187,000020454	0,000000000000867
53651,65555556	5,999996373	0,000000000001025
53652,67638889	51,000023237	0,000000000001025
53653,69583333	936,000002548	0,000000000001268
53654,72430556	35,000028298	0,000000000001025
53655,73750000	22,000015830	0,000000000001025
53656,59305556	166571,999996295	0,00000000016605
53659,41944444	501,000027847	0,000000000001382
53660,44583333	21,000002394	0,000000000001025
53661,43888889	10195,000006934	0,000000000011809
53662,04652778	25170,000119135	0,000000000022783
53663,20416667	6978,000005521	0,000000000008707
53664,29583333	0,999994576	0,000000000001025
53665,30763889	23,000216600	0,000000000001025

Table 4: Statement of the dead times of H_Maser 40 0890 - FO2 measurements between MJD 53639 to 53664

With taking $\sigma_{link\_Maser} = \sqrt{\sigma_{link\_lab}{}^2 + \sigma_{deadTime}{}^2}$ one obtains $\boxed{\sigma_{link\_Maser} = 1.431\ 10^{-16}}$

ANNEX 4

Linear Regression on the frequency measurements on period MJD 53639-53504

One calculates the linear regression by the algorithm of weighted least squares by statistical uncertainty of each frequency differences measurements:

$$y_k = a_1 + a_2\, t$$

Figure 10 gives the representation of frequency measurements and the linear fit resulting from weighted least squares by inverse of squares statistical uncertainty $1/\sigma_{Ai}^{\ 2}$.

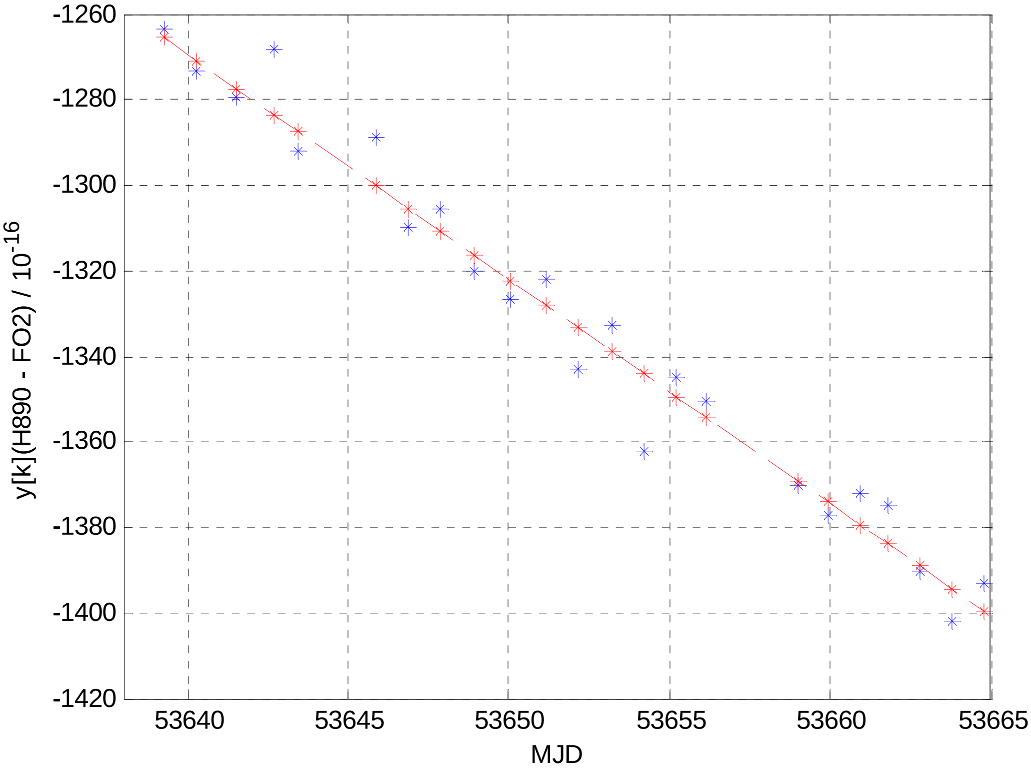

Figure 10: linear regression on the frequency y(HMaser-FO2) between MJD 53639 and 53664 weighted by uncertainty : $1/\sigma_{Ai}^{\ 2}$

Summary of statistical terms:
Coefficient a1 = 2.80422135462896e-011
Coefficient a2 = -5.25152045593957e-016
σ(a1) of y[k] FO2 = 6.16511054597299e-013
σ(a2) of y[k] FO2 = 1.14908333414611e-017

Covariance Matrix :

3.80085880440673e-025	-7.08422571100565e-030
-7.08422571100565e-030	1.32039250881233e-034

Mean date of measurements = 53652.02454861
Frequency mean by linear fit y_FO2 = -1.33256895670194e-013
Uncertainty propagation at t_moyen uc_y_FO2 = 8.71220732335572e-017
Degree of Freedom DEF = 21
Mean Square Error = Chi2/DEF = 3.05692573717004
Birge ratio Rb (chi2/DEF)^1/2 = 1.748406628096
Limit of Birge ratio Rb = 1+sqrt(2/DEF) = 1.30860669992418
Probability of a sample y(Maser-FO2) being superior of Chi2|DEF = 1.038186545423736e-006
SSR Sum Square of Residues = 1.25699366408122e-029
RMS Root Mean Square of Residues = 3.54541064487772e-015
Allan Deviation at T with assumption of White Frequency Noise = 2.04341617857297e-016
T (secondes) total duration = 2295397.00022419 seconds

High order Polynomial fit on the frequency measurements on period MJD 53639-53664

One calculates the polynomial fit order M≥2 by the algorithm of least squares on each frequency differences measurements:

$$y = \sum_{i=0}^{M} p_{i+1} \, t^{(M-i)}$$

For 23 data measurements represented on figure 11, with interval duration of 2295397 seconds during MJD 53639-53664 period. With a polynomial of order M=5 we have smoothed the maser noise on $5\tau_0$ = 498995 seconds or about 5 days. We obtain the polynomial fit represented on figure 12.

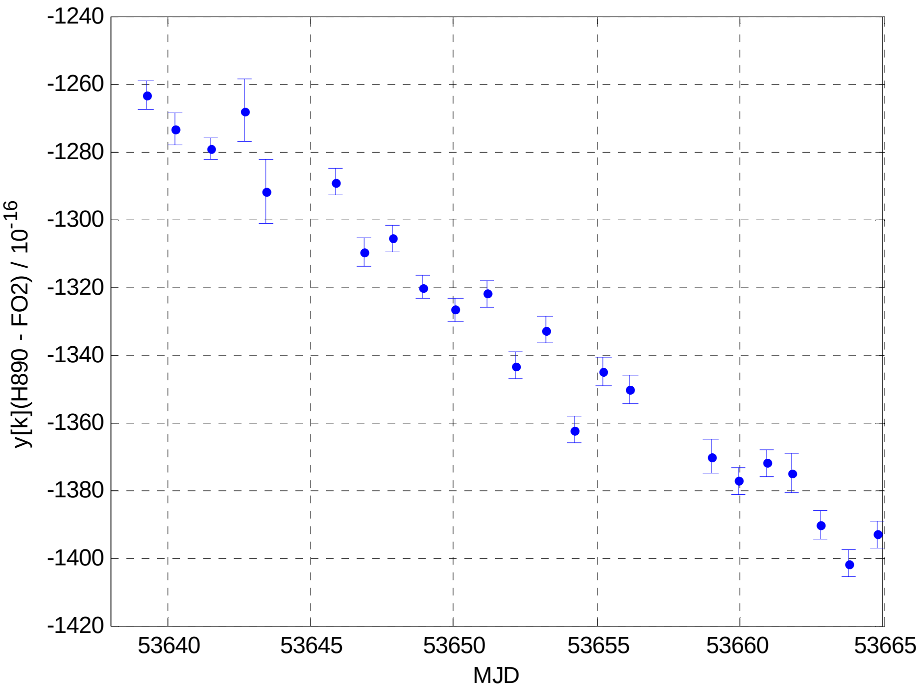

Figure 11: frequency differences & statistical uncertainties of y(H890-FO2), τ_0 = 99799s, MJD 53639 - 53664

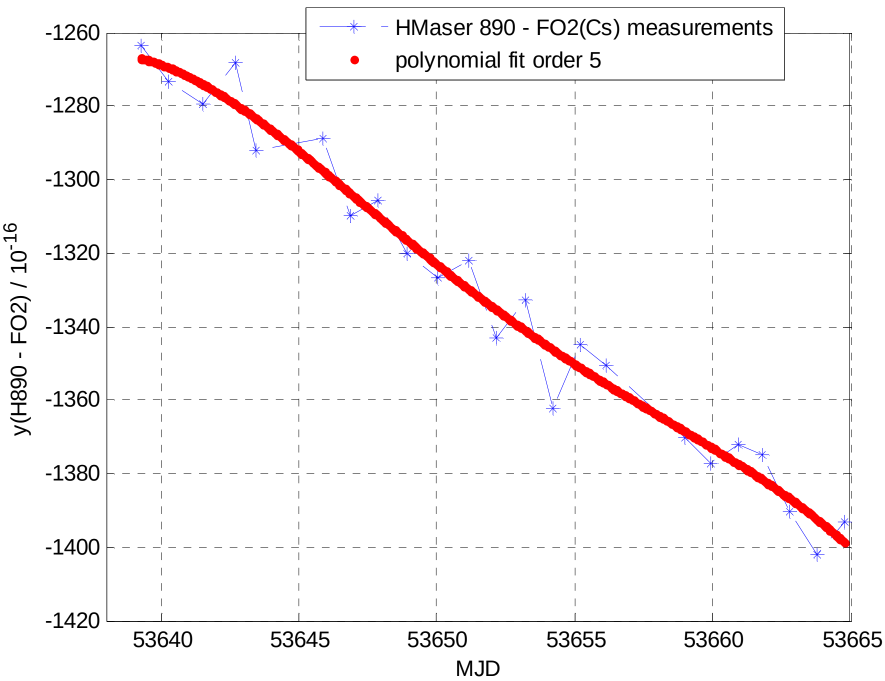

Figure 12: frequency differences y(H890-FO2) and the order 5 polynomial fit MJD 53639 - 53664

By integrating the fit polynomial from 53639 to 53664 we obtain an averaging frequency

$$y_{moy(H890-FO2)} = -1333{,}18 \times 10^{-16}$$.

Statistical uncertainty is evaluated by the frequency stability analysis of FO2 fountain. Figure 13 shows an overlapping Allan deviation for the residuals of linear fit and of polynomial fit and laws of white noise frequency modulation of 2,8 x $10^{-13}\tau^{-1/2}$modeling of Maser noise and of 2,8 x $10^{-14}\tau^{-1/2}$ modeling of fountain noise limit An extrapolated value at the total duration 26,567 days is obtained by law $\sigma_y(\tau\approx 26{,}567\ d)_{Maser}$ = 1,85 x 10^{-16} representing the instability of Maser and law $\sigma_y(\tau\approx 26.567\ d)_{FO2}$ = 1,85 x 10^{-17} representing FO2 noise with cryogenic oscillator.

By taking the fountain noise instability value extrapolated and added with the statistical uncertainty σ_A obtained from each measurement

$$\sigma_A = \sqrt{\frac{1}{\sum_{i=1}^{n} \frac{1}{\sigma_{Stat_i}^2 + \sigma_{Collision_i}^2}}}$$

resulting in σ_A = **0,706** x **10^{-16}** we finally obtain the statistical uncertainty of mean frequency **$y_{moy(H890-FO2)}$ = -1333,18 x 10^{-16}** is:

$$u_A = \sqrt{\sigma_A^2 + \sigma_y(\tau = 26.567\ d)_{FO2}^2}$$

$$\boxed{u_A := 8.9\ 10^{-17}}$$

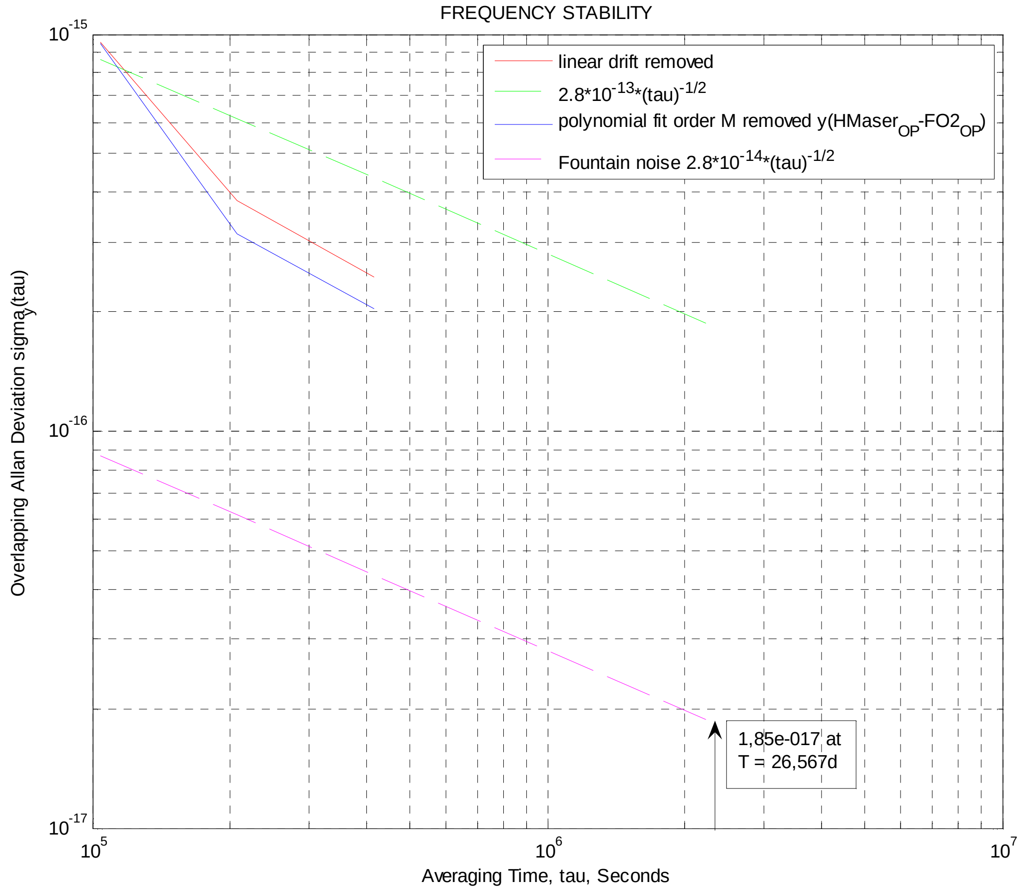

Figure 13: Comparison of frequency stability y(HMaser890 – FO2) polynomial order 1 and order M=5 removed from MJD 53639 to MJD 53664

Mean Frequency computed by phase differences

Figure 14 shows the evolution of the differences in fractional frequency y(t). At each period of integration is evaluated a frequency $\tilde{y}_k$ corresponding to the interval $t_{k+1} - t_k$. The relation binding the variations of phase and the instantaneous frequency deviations is given by

$$y_k = \frac{x_{k+1} - x_k}{t_{k+1} - t_k} \quad (1)$$

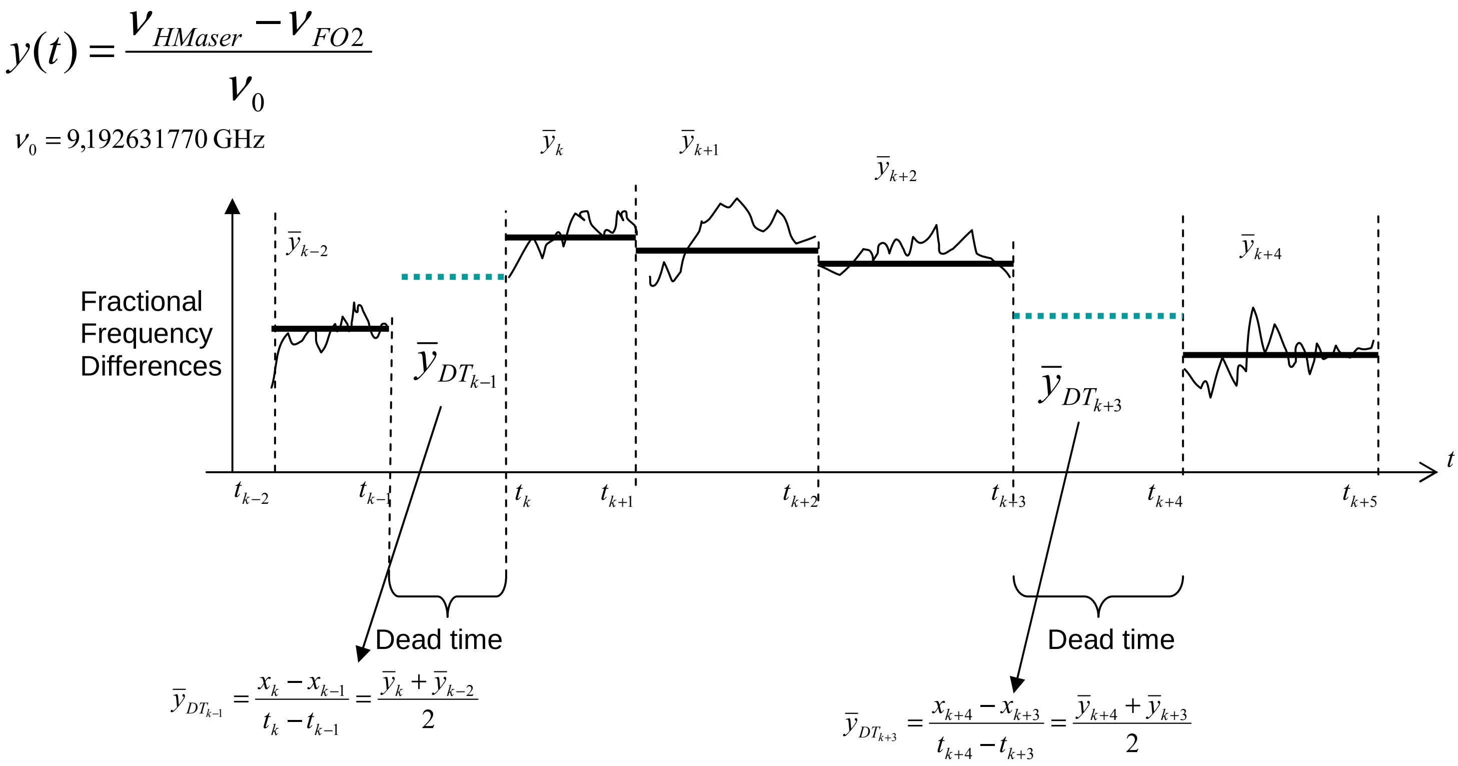

Figure 14: contribution of frequency measurements on the mean frequency calculated

By using equation (1) we have $x_{k+1} - x_k = (t_{k+1} - t_k)\, y_k$

and for addition of consecutive phase differences we find $\sum_{k=1}^{N} (x_{k+1} - x_k) = x_{N+1} - x_1 = \sum_{k=1}^{N} (t_{k+1} - t_k)\, y_k$

During the dead time we have evaluated the mean frequency by interpolating the mean frequency between two neighbouring intervals of integrations noted:

$$y_{DT_{m-1}} = \frac{1}{2} y_m + \frac{1}{2} y_{m-1} \quad (2)$$

The contributions of N duty intervals with the frequency measurements y_k and *M* idle intervals with the mean frequency extrapolating between two neighbouring intervals of integration y_{DT} give the summation

$$\left(\sum_{k=1}^{N} (t_{k+1} - t_k)\, y_k \right) + \left(\sum_{m=1}^{M} (t_{m+1} - t_m)\, y_{DT_m} \right) = x_{fin} - x_{deb} \quad (3)$$

$$\boxed{y_{moy} = \frac{x_{fin} - x_{deb}}{86400\ MJD_{fin} - 86400\ MJD_{deb}}} \quad (4)$$

Where ($x_{fin} - x_{deb}$) represents the phase variation between the whole period of integration.

The evaluation of statistical uncertainty on each phase differences data extracted from fractional frequency differences, as we have in presence of white frequency noise (WFM) in each period of measurement, is given by the expression

$$\sigma_x(\tau_i)^2 = \sigma_y(\tau_i)^2\,\tau_i^2$$

For the whole period T of measurement that gives in frequency instability

$$\sigma_y(\tau = T) = \sum_{i=1}^{23} \frac{\sqrt{\left(\sigma^2_{Stat_i} + \sigma^2_{Collision_i}\right)\,\tau_i^2}}{T}$$ (See table 2 for σ_{Stat} and $\sigma_{Collision}$).

With N =23, from the 10th September to 4th November 2005 and $T = 86400\ MJD_{fin} - 86400\ MJD_{deb}$ = 2295397 seconds it gives

$\sigma_y(\tau = T) = 7.061\ 10^{-17}$ ➔ $\boxed{\sigma_A = 7.061\ 10^{-17}}$

The evaluation of the mean frequency between two intervals of integrations during the period from MJD 53639 to MJD 53664 is given by equation (2) and calculated for frequency fluctuation difference measurements. Figure 15 shows the frequency differences between H_Maser 40 0890 and FO2 (blue plus) and the mean frequency during dead times (magenta stars).

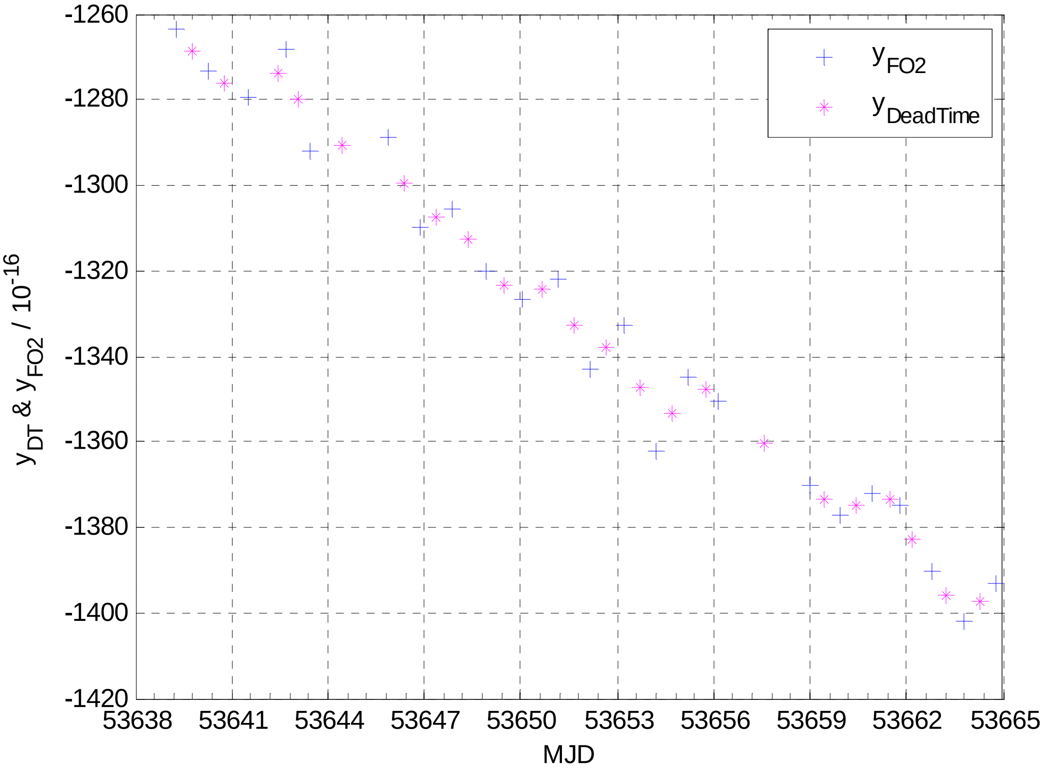

Figure 15: frequency differences H_Maser40 0890 and FO2 from MJD 53639 up to MJD 53664

From equation (3) we find the phase difference over the whole period of integration

$$x_{fin} - x_{deb} = -305.7642 \text{ ns}$$

This value is replaced in equation (4) above for computation of y_{moy} during this period. We find

$$\boxed{y_{moy} = -1.33208\ 10^{-13}}$$

REFERENCES

[ref. 1] - C. Vian, P. Rosenbusch, H. Marion, S. Bize, L. Cacciapuoti, S. Zhang, M. Abgrall, D. Chambon, I. Maksimovic, P. Laurent, G. Santarelli, A. Clairon of Obs. Paris, SYRTE, A. Luiten, M. Tobar, Univ. W. of Australia School of Physics, C. Salomon of LKB, "LNE-SYRTE Fountains: Recent Results", **CPEM 2004, Proceedings IEEE Transactions on Instrumentation & Measurement, Vol. 54, N0. 2, April 2005.**

[ref. 2] - F. Pereira Do Santos, H. Marion, M. Abgrall, S. Zhang, Y. Sortais, S. Bize, I. Maksimovic, D. Calonico, J. Grünert, C. Mandache, C. Vian, P. Rosenbusch, P. Lemonde, G. Santarelli, Ph. Laurent and A. Clairon of LNE-SYRTE, C. Salomon of LKB, "Rb and Cs Laser Cooled Clocks: Testing the Stability of Fundamental Constants". **Proceedings IEEE 2003, EFTF Tampa May 2003, p 55-67.**

[ref. 3] - P. Wolf of LNE SYRTE, C.J. Bordé of LPL, "Recoil effects in microwave Ramsey spectroscopy", arxiv: **quant-ph/0403194**.

[ref. 4] - F. Pereira Do Santos, H. Marion, S. Bize, Y. Sortais, A. Clairon, and C. Solomon "Controlling the Cold Collision Shift in High Precision Atomic Interferometry" of, **Phys, Rev, Lett, 89,233004 (2002)**.

[ref. 5] - J. Vanier, C. Audouin, « The Quantum Physics of Atomic Frequency Standards », **Adam Hilger, Bristol & Philadelphia (1989)**.

[ref. 6] - R. Schröder, U. Hübner and D. Griebsch, "Design and Realization of the Microwava Cavity in PTB Caesium Atomic Clock CSF1" **IEEE Trans. Instrum. Meas., vol. 49, p.383, 2002**.

[ref. 7] - L. Cutler *et al*, "Frequency pulling by hyperfine σ - transitions in cesium atomic frequency standards, **J. Appl. Phys. Vol. 69, pp. 2780, 1991**.

[ref. 8] - A. Bauch, R. Schröder "Frequency shift in Caesium Atomic Clock due to Majorana transitions", Annalen der Physik**, vol. 2, pp. 421, 1993**.

[ref. 9] – H. Marion thèse de doctorat de l'Université de Paris 6 (Mars 2005)

[ref. 10] - E. Simon, P. Laurent, and A. Clairon, Measurement of the Stark shift of the Cs hyperfine splitting in an atomic fountain, PRA vol.57 p.436 (1998)

[ref. 11] - Wayne M. Itano and D. J. Wineland, Laser cooling of ions stored in harmonic and Penning traps, PRA vol.25, p.35 (1982)

[ref. 12] - V G Pal'chikov *et al,* Black-body radiation effects and light shifts in atomic frequency standards *J. Opt. B: Quantum Semiclass. Opt.* **5** S131-S135 (2003)